arXiv:0912.1088v1 [cond-mat.quant-gas] 6 Dec 2009

High Order Momentum Modes by Resonant Superradiant Scattering

Xiaoji Zhou,* Jiageng Fu, and Xuzong Chen
School of Electronics Engineering & Computer Science, Peking University, Beijing 100871, China

The spatial and time evolutions of superradiant scattering are studied theoretically for a weak pump beam with different frequency components traveling along the long axis of an elongated Bose-Einstein condensate. Resulting from the analysis for mode competition between the different resonant channels and the local depletion of the spatial distribution in the superradiant Rayleigh scattering, a new method of getting a large number of high-order forward modes by resonant frequency components of the pump beam is provided, which is beneficial to a lager momentum transfer in atom manipulation for the atom interferometry and atomic optics.

PACS numbers: 03.75.Kk, 42.50.Gy, 32.80.Lg

I. INTRODUCTION

Atom interferometry is a valuable tool for studying scientific and technical fields such as precision measurements and quantum information, and a very bright source is Bose-Einstein Condensate (BEC) of atomic gases. In which an important technique is to manipulate the translational motion of atoms and transfer atoms coherently between two localities in position and momentum [1]. To obtain the momentum transfer, one useful method is two-photon Bragg diffraction, where two laser beams impinge upon atoms, whose atoms can undergo stimulated light-scattering events by absorbing a photon from one of the beams and emitting into the other. The momentum transfer is determined by the difference in the wave vectors of the beams, and the frequency difference defines the corresponding energy transfer [2]. We will introduce another method to obtain a large number of high-order momentum modes by the resonant superradiant scattering from a BEC for a weak pump beam with several frequency components.

A typical superradiance experiment consists in a far off-resonant laser pulse traveling along the short axis of a cigar-shaped BEC sample [3], the scattered lights, called end-fire modes, propagate along the long axis of the condensate, and the recoiled atoms are refereed to as side modes. A series of experiments [4, 5, 6, 7, 8] have sparked related interests in phase-coherent amplification of matter waves [4, 5], quantum information [6], collective scattering instability [7], and coherent imaging [8]. Several theoretical descriptions of these cooperative scattering in BEC with single-frequency pump have also been presented [9, 10, 11, 12].

For the long and weak pump beam, we can observe the forward peaks correspond to Bragg diffraction of atoms [3], where the high order scattering is limited by detuning barriers for the end-fire mode radiation [13]. On the other hand, a X-shaped recoiling pattern is demonstrated in a short and strong pulse as Kapitza-Dirac diffraction of atoms [4], where an atom in the condensate absorbs a photon from the pump laser, then emits a photon into an end-fire mode, and recoils forwardly. Meanwhile another atom absorbs a photon from the end-fire modes, emits into the pump beam and finally recoils backwardly. In this case, there is an energy mismatch of four times the one-photon recoil kinetic energy $\hbar\omega_r$ in backward scattering, which then remains very weak unless a short pumping pulse with a broad spectrum is used. Hence, two phase-locked incident lasers with the frequency difference $\Delta\omega$ compensating for the energy mismatch has been used [6, 14, 15], which is named resonant superradiance, where a large number of backward recoiling atoms can be produced.

Followed that, it is attractive to extent this idea to achieve a high momentum transfer by overcoming the detuning barriers, by a weak and long pump beams with the resonant frequency. It requires to analysis the competition between the different transition channels and the spatial distribution of different modes. Because the above traditional superradiant-scattering configuration involves many atomic side modes coupled together, to simplify it, we chose another configuration where a pump beam travels along the long axis of the BEC. This scheme is widely studied in photon echo [16], decoherence [17], spatial distribution effects [18] and self-organized formation of dynamic gratings [19]. Since the pulse length is far longer than the initial spontaneous process [11], we choose the semi-classical theory which can well describe the experimental results [6, 11, 14].

In this paper, we first introduce the semi-classical theory for the superradiance scattering with a several-frequency pump in the weak coupling. Then the spatial and time evolutions of scattered modes are analyzed for one-frequency pump beam. Followed that, in the case of two-frequency pump, we find the backward first order scattering mode is suppressed at the resonant condition $\Delta\omega = 8\omega_r$ and the forward second order mode is enhanced, resulting from the combination of mode competition effects and spatial distribution of the modes. The case of the three-frequency pump beams for a lager number of the forward third order scattering modes, and the higher modes for more resonant frequencies are studied, which supplies a new method to get a large number of atoms in higher order forward modes. Finally, some discussion and conclusion are given.

---

*Electronic address: xjzhou@pku.edu.cn

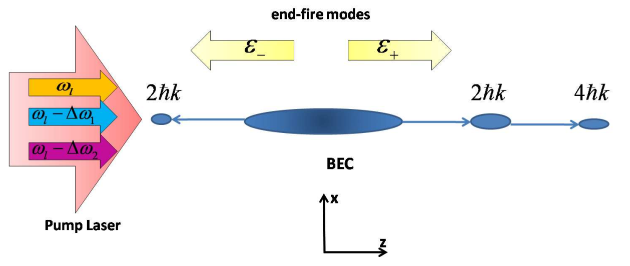

FIG. 1: (Color online) Our experimental scheme. A cigar-shape BEC is illuminated by a far off-resonant laser pulse along its long axis $\hat{\mathbf{z}}$. Collective Rayleigh scattering induces superradiance. Two end-fire modes, which are also along $\hat{\mathbf{z}}$ axis, form in superradiance process and the 1st-order recoiled atoms obtain a momentum of $2\hbar\mathbf{k}$.

II. MODEL FOR A MULTIPLE-FREQUENCY END-PUMPED BEAM

We consider the pump laser, with amplitude $\mathcal{E}_l(t)$, polarization $\mathbf{e_y}$, wave vector $\mathbf{k_l}$, frequencies ω_l and $\omega_l-\Delta\omega_n$, propagating along the long axis $\hat{\mathbf{z}}$ of an elongated BEC, $\mathbf{E}_l = \mathcal{E}_l(t)\mathbf{e_y}[(1+\Sigma_n e^{i\Delta\omega_n t})e^{i(k_l z-\omega_l t)} + c.c.]/2$, as shown in Fig. 1. When supperradiant Rayleigh scattering happens, end-fire modes spread along the same axis. The $\mathcal{E}_+$ mode has the same direction as the incident light and mainly interacts with the right part of the condensate, and the $\mathcal{E}_-$ mode overlaps with the left part of the condensate. The atoms are recoiled to some discrete momentum states with momentum $2m\hbar\mathbf{k}$, where m is an integer and the wave vector of end-fire mode light k is approximated as k_l for energy conservation. The total electric field $\mathbf{E}(\mathbf{r},t)=\mathbf{E}^{(+)}+\mathbf{E}^{(-)}$ is given by [6, 11, 14, 18]

$$\begin{aligned}\mathbf{E}^{(+)}(\mathbf{r},t) &= [(1+\sum_n e^{i\Delta\omega_n t})\mathcal{E}_l(t)e^{-\mathrm{i}(\omega_l t-k_l z)}/2 \\ &+ \mathcal{E}_-(z,t)e^{-\mathrm{i}(\omega t+kz)}]\mathbf{e_y} \qquad (1)\end{aligned}$$

where $\omega=ck$, $\mathbf{E}^{(-)}=\mathbf{E}^{(+)*}$, and $\mathcal{E}_+$ is ignored because it has the same wave vector as the pump beam but is very small in comparison to $\mathcal{E}_l$. $\Delta\omega_n$ satisfies the condition $\Delta\omega_n \ll \omega_l$ [6] and the initial phases of the different frequency components are assumed to be zero.

Since the BEC is tightly constrained in its short axis ($\hat{\mathbf{x}}$, $\hat{\mathbf{y}}$) in the present superradiance setup and the Fresnel number of the optical field is around 1, one dimensional approximation is usually used [3, 6, 18, 19]. We expand the wavefunction of the condensate $\psi(\mathbf{r},t)$ in momentum space, $\psi(\mathbf{r},t) = \sum_m \phi_m(z,t)e^{-\mathrm{i}(\omega_m t-2mkz)}$, where $\phi_m(z,t)=\psi_m(z,t)/\sqrt{A}$, $\omega_m = 2\hbar m^2k^2/M$, $m=0$ corresponds to the residual condensates, $m\neq 0$ denotes the side modes, and A is the average cross area of the condensate perpendicular to $\hat{\mathbf{z}}$. Using the Maxwell-Schrödinger equations, we obtain dynamics equations for $\phi_m(z,t)$,

$$\begin{aligned}\mathrm{i}\frac{\partial\phi_m}{\partial t} &= -\frac{\hbar}{2M}\frac{\partial^2\phi_m}{\partial z^2}-\frac{2\mathrm{i}m\hbar k}{M}\frac{\partial\phi_m}{\partial z} \\ &+ \bar{g}\left[\mathcal{E}_-^*\phi_{m-1}e^{-4\mathrm{i}(1-2m)\omega_r t}+\mathcal{E}_-\phi_{m+1}e^{-4\mathrm{i}(1+2m)\omega_r t}\right], \qquad (2)\end{aligned}$$

where $\omega_r=\hbar k_l^2/2M$ is the recoil frequency, the coupling between modes is given by

$$\bar{g}(t) = g\left(1+\sum_n e^{i\Delta\omega_n t}\right), \qquad (3)$$

with the coupling factor $g=\sqrt{3\pi c^3 R/(2\omega_l^2 AL)}$, R is the Rayleigh scattering rate of the pump components, and L is the BEC length.

The first term on the right-hand-side of Eq.(2) describes the dispersion of ϕ_m, and the second term gives rise to their translation. The terms in square brackets describe the atom exchange between ϕ_m and ϕ_{m+1} or ϕ_{m-1} through the pump laser and end-fire mode fields. An atom in mode m may absorb a laser photon and emit it into end-fire mode $\mathcal{E}_-$, and the accompanying recoil drives the atom into $m+1$ mode, hence atoms with mode $m+1$ can emerge in forward scattering. On the other hand, in the backward scattering, atoms with mode m absorb one $\mathcal{E}_-$ mode photon, deposit it into the laser mode and go into mode $m-1$. The envelope function of end-fire mode $\mathcal{E}_-$ is given by

$$\mathcal{E}_- = -\mathrm{i}\frac{\omega_r\bar{g}}{2c\varepsilon_0}\int_z^{+\infty}\mathrm{d}z'\sum_m \phi_m(z',t)\phi_{m+1}^*(z',t)e^{\mathrm{i}4(2m+1)\omega_r t}, \qquad (4)$$

indicating that the end-fire mode field $\mathcal{E}_-$ is due to the transition between m and $m+1$ mode and the magnitude of $\mathcal{E}_-$ depends on the spatial overlap between the two modes. In addition, there is a frequency difference of $8\omega_r$ between adjacent modes.

III. THE SPATIAL AND TIME EVOLUTION OF SCATTERED MODES WITH A SINGLE-FREQUENCY PUMP BEAM

For explaining effects of spatial distribution and the depletion mechanism in the scattering from BEC, we first study the case of a single-frequency pump in the weak coupling regime. The evolution of spatial distribution of atomic side modes and optical end-fire mode are depicted in Fig.2, where the original BEC is assumed to be symmetrical.

Superradiance first starts at the leading-edge of the BEC, as shown in Fig.2 (a). The end-fire mode $\mathcal{E}_-$ monotonically increases at the beginning and becomes strong on the side of the end-pump, and it has a large overlap with the BEC. The atomic side modes and the optical-field modes are well localized at the condensate edge. Hence, the recoiled atoms mainly come from this edge of the condensate, and the forward first order mode $m=1$ emerges due to the overlap between the condensate at $m=0$ and the end fire mode $\mathcal{E}_-$. Then at some point the condensate is completely scattered to mode $m=1$ and the atoms are transferred back to the edge, leading to a minimum in the condensate density and regrowth at the edge, as shown in Fig.2 (b), which appears like a Rabi oscillation between the condensate and first-order side mode. When the overlap between mode $m=0$ and $\mathcal{E}_-$ is significantly large, the minimum point of mode $m=0$ and the peak of mode

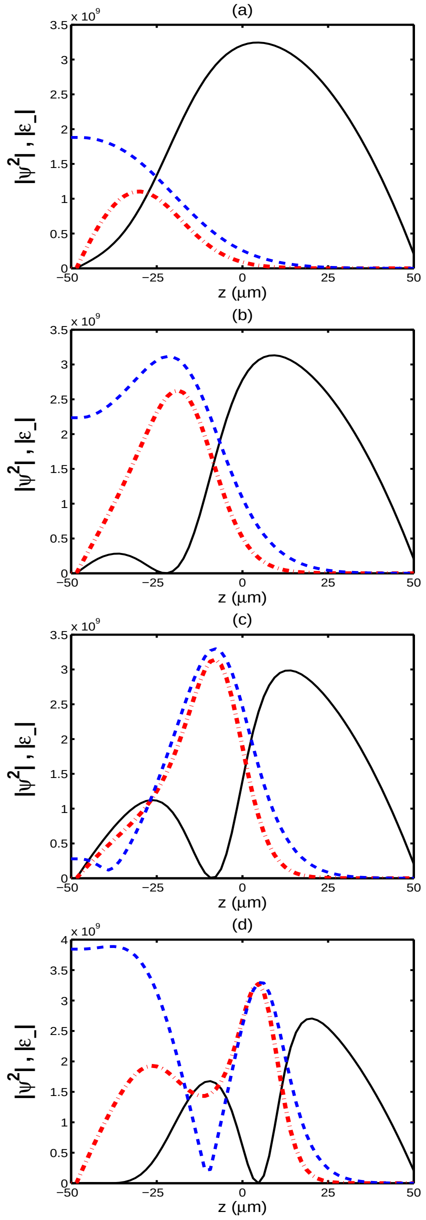

FIG. 2: (Color online) Spatial distribution of the atomic side modes $|\psi^2|$ and the light end-fire mode $|\varepsilon_-|$ in the weak coupling ($g = 1.25\times10^6 s^{-}1$) in case of a single-frequency pump for different pulse durations: 150us (a); 200us (b); 250us (c); 350us (d). The condensate mode $m = 0$ is the solid line, the forward first-order side mode $m = 1$ is the dash-dotted line, and the end-fire mode is the dashed line.

$m = 1$ move from the leading-edge to the center of the BEC, as shown in Fig.2 (c). When the regrowth part of mode $m = 0$ is comparable to mode $m = 1$, it will be scattered to mode $m = 1$ again. Hence mode $m = 1$ also has an edge regrowth. Due to the movement of the first peak and the regrowth from the edge, mode $m = 1$ will have a minimum point too, as shown in Fig.2 (d). This distribution shows the evolution of side modes in space and the absence of backward-scattering modes in the weak coupling regime.

The distribution of the first-order side mode closely connects with the end-fire mode, and $\mathcal{E}_-$ is simply the result of the coupling between ϕ_0 and ϕ_1. When the condensate population at some point z is completely pumped to the first-order side mode, the population of mode $m = 1$ and $\mathcal{E}_-$ are at maximum. When the first-order side mode absorbs end-fire mode photons leading to the regrowth of the condensate, the populations of mode $m = 1$ and $\mathcal{E}_-$ will reach minimum. The asymmetry could be explained by Eq.(2), where ϕ_0 and ϕ_1 are coupled through $\mathcal{E}_-$ which is very small at the tailing-edge of the condensate.

The evolution of the side modes and the end-fire mode indicates that the scattering is a localized process. In this end-pumping configuration, the scattering first starts on the leading edge of the BEC and then moves towards the tailing edge.

IV. MODE COMPETITION FOR A TWO-FREQUENCY PUMP BEAM

To investigate the effect of the two-frequency pump beam in the case of end-pumping, the different frequency components of the end-fire mode which indicate the energy change during the scattering are depicted in Fig. 3. The momentum of side mode $m = n$ is $2n\hbar\mathbf{k}$, and its kinetic energy is $4n^2\hbar^2\mathbf{k}^2/2M = 4n^2\hbar\omega_r$. For the pump component with frequency ω_l, atoms from the condensate are pumped to the side mode $m = 1$ and emit end-fire mode photons with frequency $\omega_l - 4\omega_r$ spontaneously. However, in the backward scattering process, an atom in the condensate absorbs the end-fire mode ($\omega_l - 4\omega_r$) and emits a photon with frequency ω_l back into the pump laser. Since energy is not conserved in backward-scattering, the backward side mode is not populated in weak-pulse regime. Side mode $m = 2$ is also not populated due to the energy barrier. However, if we use the two components pump laser with frequency difference $8\omega_r$, i.e. resonant frequency difference, the energy mismatch can be compensated by the pump laser.

Although the resonant condition for the backward mode is satisfied, it should be noticed that two scattering channels exist almost simultaneously. One is atoms scattered from side mode $m = 0$ to $m = -1$ and the other is from $m = 1$ to $m = 2$, resulting in mode competition. The transition from mode $m = 1$ to $m = 2$ requires absorbtion of photons from pump laser, while the backward transition takes photons from the end-fire mode. Because the intensity of the pump laser is far greater than that of the end-fire mode, the transition from $m = 1$ to $m = 2$ has a bigger probability than the transition from $m = 0$ to $m = -1$. Thus the population of the backward mode $m = -1$ is suppressed even at the resonant condition, while the forward mode $m = 2$ is enhanced.

However, the existence of competition between these two channels may not lead to the suppression of the backward mode. If these two channels happen in different spacial parts of the condensate, then both of side mode $m = -1$ and $m = 2$ will be enhanced. The suppression of backward mode $m = -1$ and the enhancement of mode $m = 2$ need that these two scat-

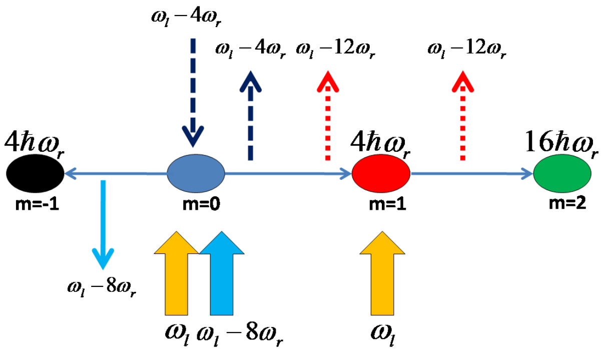

FIG. 3: (Color online) Light-field components of a two-frequency pump laser. The broad arrows are the pump laser and narrow ones are the end-fire mode (scattering optical field). In a spontaneous process, atoms in the condensate absorb photons from the pump laser with frequencies ω_l and $\omega_l - 8\omega_r$, are scattered to side mode $m = 1$ and emit end-fire mode photons with frequency $\omega_l - 4\omega_r$ (dashed arrow) and $\omega_l - 12\omega_r$ (dotted arrow), respectively. Meanwhile, atoms in the condensate can also absorb end-fire mode photons with frequency $\omega_l - 4\omega_r$, be scattered back to side mode $m = -1$ and emit photons with frequency $\omega_l - 8\omega_r$(solid arrow), resonating to one of the pump laser components. The side mode $m = 1$ can absorb pump laser photons with frequency ω_l and be scattered to mode $m = 2$, emitting photons with frequency $\omega_l - 12\omega_r$ resonating to the existing end-fire mode.

tering channels happen in the same area. Therefore, the spatial distribution effect should be considered.

We analyze the spatial effect when second-order forward side mode and backward side mode are populated at the resonant condition $\Delta\omega = 8\omega_r$. The evolution of spatial distribution of side modes and end-fire mode is shown in Fig.4. Superradiance first starts on the leading edge of the BEC, as shown in Fig.4(a). Although the backward first-order side mode $m = -1$ is populated through the overlap between end-fire mode $\mathcal{E}_-$ and side mode $m = 0$, it is very small and emerges at the leading-edge of the BEC. Since the overlap between end-fire mode and side mode $m = 1$ is in the same area, the population of side mode $m = 2$ is obvious on this edge, as shown in Fig.4(b). Side mode $m = 2$ grows more rapidly than side mode $m = -1$, which means more atoms are scattered from side mode $m = 1$ to $m = 2$ than that from $m = 0$ to $m = -1$.Then the first peaks of side modes $m = 1$ and $m = 2$ move to the center of the BEC, as shown in Fig.4(c). Though the movement of the peaks is similar to that in the case of a single-frequency pump laser, one major difference is that the regrowth of side mode $m = 0$ is very little, hence nearly all the atoms on this edge are forwardly scattered. Due to the nearly-complete depletion of the condensate, atoms are mainly transferred between side mode $m = 1$ and $m = 2$. The apparent regrowth of side mode $m = 1$ on the leading-edge shown in Fig.4(d) indicates that there are Rabi oscillations between side modes $m = 1$ and $m = 2$ in the depleted area of the condensate.

The above phenomenon is different from the case of the pump laser traveling along the short axis. In the latter case, a correlation between the center depletion of the BEC and backward mode was reported in Ref. [11]. However, in our case, such correlation does not exist because side mode $m = 2$ emerges on the edge of the BEC. As a consequence of the edge depletion of the BEC, backward side mode $m = -1$ is not populated significantly, because the end-fire mode mainly distributes in the leading edge where side mode $m = 0$ suffers the

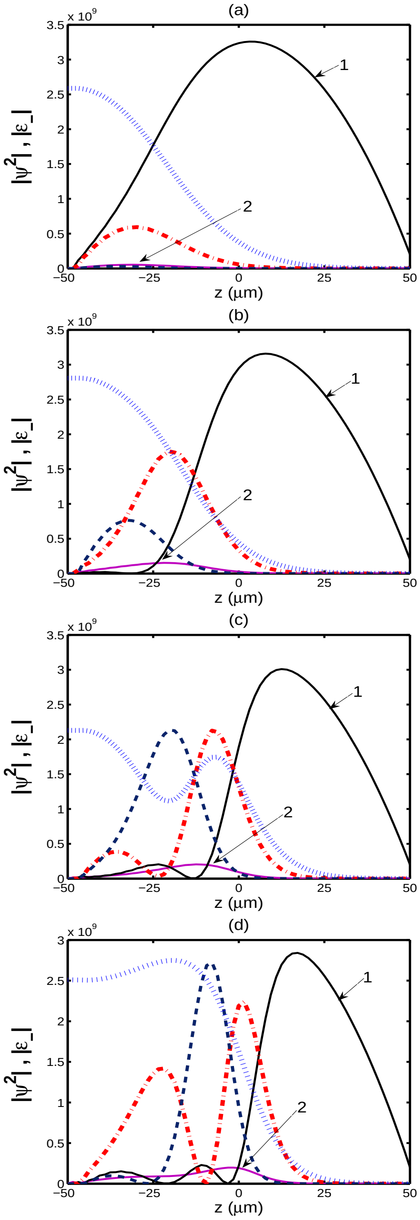

FIG. 4: (Color online) Spatial distribution of the side modes $|\psi^2|$ and the end-fire mode $|\varepsilon_-|$ in the weak coupling regime ($g = 1.25 \times 10^6 s^-1$) with the two-frequency pump for different pulse durations: 150us (a); 200us (b); 250us (c); 300us (d). Condensate mode $m = 0$ is the solid line-1, backward first-order side mode $m = -1$ is the solid line-2, forward first-order side mode $m = 1$ is the dash-dotted line, forward second-order side mode $m = 2$ is the dashed line, and end-fire mode is the dotted line.

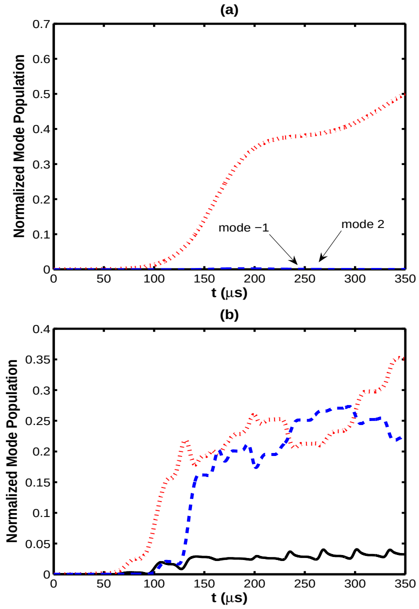

FIG. 5: (Color online) Normalized side mode populations versus time: (a) for a single-frequency pump beam; (b) for a two-frequency resonant pump beam. In both cases the coupling constant is kept $g = 1.55 \times 10^6 s^{-1}$. The side mode are: m=-1 (solid); m=1 (dotted); m=2 (dashed).

strongest depletion. Thus only a small number of atoms in the residual condensate can absorb end-fire mode photons and be scattered backwardly. In another word, the emergence of side mode $m = 2$ suppress backward-scattering atoms. Therefore the efficiency of getting $m = 2$ mode with this two-frequency pump is strongly enhanced while greatly suppressed for the backward side mode.

The time evolution of several side modes populations normalized by the total atom number are depicted by Fig.5. Fig.5 (a) shows that using a single-frequency pump laser cannot produce backward mode $m = -1$ or forward higher mode $m = 2$ in the weak-pulse regime. Using a resonant two-frequency pump beam with the same intensity, modes $m = -1$ and $m = 2$ increased, as shown in Fig.5 (b), however, the forward mode is greatly enhanced while the backward mode remains very small.

V. THE THIRD ORDER FORWARD MODES ENHANCED WITH A THREE-FREQUENCY PUMP BEAM

The second forward side mode $m = 2$ is greatly enhanced with a resonant two-frequency pump beam, however, the populations of higher forward modes such as $m = 3$ are very small as the channel from the second forward mode to the third forward mode is not resonant with the exiting optical field. To get a large number mode for $m = 3$, Fig.6 depicts the scheme of the three-frequency pump beam with the frequencies of the pump laser ω_l, $\omega_l - 8\omega_r$ and $\omega_l - 16\omega_r$. The frequency components ω_l, $\omega_l - 8\omega_r$ and $\omega_l - 16\omega_r$ both have the resonant frequency difference. Hence, there could be two channels to form the backward side mode $m = -1$ but the enhancement of the backward scattering is small because of the formation of higher forward side modes. There are also two channels to form side mode $m = 2$. One thing different from the two-frequency pump beam is that there is also a channel to form side mode $m = 3$ for the reason that atoms in side mode $m = 2$ absorb pump laser photons with frequency ω_l, are then scattered to mode $m = 3$ and eventually emit end-fire mode photons with frequency $\omega_l - 20\omega_r$ which is resonant to an existing end-fire mode. This means that more atoms in side mode $m = 2$ will be pumped to side mode $m = 3$ and less will be transferred back to side mode $m = 1$, a competition between side mode $m = 3$ and $m = 1$ is set up. As a result, side mode $m = 3$ will be enhanced and $m = 1$ will be reduced relatively.

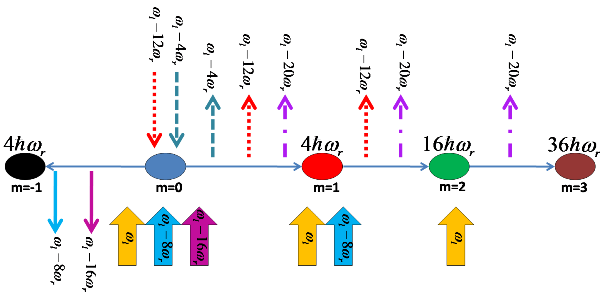

FIG. 6: (Color online) The light-field components of a three-frequency pump laser. The broad arrows are the pump laser and narrow ones are the end-fire mode.

Fig.7(a) is the simulated result of the time evolution of normalized side mode populations for a three-frequency pump beam. We could see that side mode $m = 3$ would be strongly enhanced at long time while side mode $m = 1$ reduced.

VI. MOMENTUM TRANSFER IN THE HIGH ORDER FORWARD MODES

From the above discussion we know that using multi-resonant frequencies is a promising way to get a large number of higher forward modes. When a pump laser has frequency components $\omega_l, \omega_l - 8\omega_r, \cdots, \omega_l - (n-1) * 8\omega_r$, satisfying $(n-1) * 8\omega_r \ll \omega_l$, with the kinetic energy of mode $m = n$ equal to $4n^2\hbar\omega_r$, then after the condensate atoms spontaneously scattered to mode $m = 1$, the end-fire mode will have frequency components $\omega_l - 4\omega_r, \omega_l - 12\omega_r, \cdots, \omega_l - (2n-1) * 4\omega_r$. For resonance concern, mode $m = 1$ will absorb photons from the pump components $\omega_l, \omega_l - 8\omega_r, \cdots, \omega_l - (n-2) * 8\omega_r$ and emits end-fire mode photons with frequency $\omega_l - 12\omega_r, \cdots, \omega_l - (2n-1) * 4\omega_r$ which are resonant with existing end-fire mode, so mode $m = 2$ is produced. Like mode $m = 1$, modes $m = 2, m = 3, \cdots, m = n - 1$ can absorb pump photons and emit photons resonant to the existing end-fire mode. For example, mode $m = n - 1$ will absorb photons with frequency ω_l and emits photons with frequency $\omega_l - (2n - 1) * 4\omega_r$. Therefore atoms could finally be transferred to mode $m = n$. Note

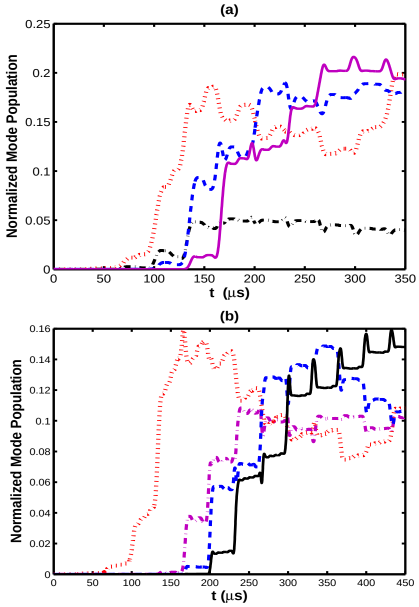

FIG. 7: (Color online) Normalized side mode populations versus time with the coupling constant $g = 1.55 \times 10^6 s^{-1}$: (a) for a three-frequency pump laser: $m = -1$ (dash-dotted), $m = 1$ (dotted), $m = 2$ (dashed), $m = 3$ (solid) ; (b) for a five-frequency pump laser: $m = 1$ (dotted), $m = 3$ (dash-dotted), $m = 4$ (dashed), $m = 5$ (solid) .

that mode $m = n$ cannot emit resonant end-fire mode, so mode $m = n$ will be enhanced. To show it, Fig.7(b) is the simulated result of the time evolution of normalized side mode populations for a five-frequency pump beam. We could see that side mode $m = 5$ would be strongly enhanced.

VII. DISCUSSION AND CONCLUSION

In the experiment, to get several resonant frequencies, the laser beam from an external cavity diode laser can be split into several parts, and their frequencies are shifted individually by acoustic-optical modulators (AOMs) which are driven by phase-locked radio frequency signals, as demonstrated in the case of two resonant frequency [6, 14]. Therefore, the frequency difference between the beams can be controlled precisely. Furthermore, to avoid the reflection from the glass tube and formation of Bragg scattering in the experiment, the pump beam can actually deviate a few degrees from the long axis, as shown in the experiments [17, 18, 19].

Different to the works in the configuration where the pump beam travels along the short axis of the condensate with the resonant frequency [14], where a large number of backward scattering is obvious in a two-frequency pump beam, the backward scattering is suppressed and the forward second-order mode is obviously enhanced in our case. This is due to mode competition between the forward second-order mode and the backward mode and local depletion of the superradiant process.

We have not considered the initial quantum process because its time scale is very small, shorter than $1\mu s$. In this quantum process there is also mode competition to form the end-fire modes along the long axis and suppress the emission on the other direction. This is different concept from what has been discussed above, in which case mode competition exists in the different channels satisfying the energy match and spatial condition.

For the pump beam with several resonant frequencies, not only can we obtain the high order momentum transfer which is important in the momentum manipulation for atom interferometry, but also the above analysis is useful to understand the interplay between the matter wave and light in the matter wave amplification [4, 5], atomic cooperative scattering in the optical lattice [20], and by the pump with a noisy laser [21, 22].

In conclusion, superradiant scattering from BEC is studied with incident light having different frequency components traveling along the long axis of the BEC in the weak coupling regime. It provides a method to get high forward modes by adding different frequency components to the pump beam. This is the result of both mode competition for the concern of energy and the local depletion of the spatial distribution. Our results shows that the spatial effects and mode competition are very important even in the case of resonant superradiance.

We thank Thibault Vogt, Lan Yin for critical reading of the manuscript and comments. Thank L. You for his helpful discussion. This work is partially supported by the state Key Development Program for Basic Research of China (No.2005CB724503, and 2006CB921402,921401), and by NSFC (No.10874008, 10934010 and 60490280).

---

[1] A. D. Cronin, J. Schmiedmayer, D. E. Pritchard, Rev. Mod. Phys. **81**, 1051(2009).
[2] A. Brunello, F. Dalfovo, L. Pitaevskii, S. Stringari, and F. Zambelli, Phys. Rev. A **64**, 063614 (2001).
[3] S. Inouye, A. P. Chikkatur, D. M. Stamper-Kurn, J. Stenger, D. E. Pritchard, and W. Ketterle, Science **285**, 571 (1999).
[4] D. Schneble, Y. Torii, M. Boyd, E. W. Streed, D. E. Pritchard, and W. Ketterle, Science **300**, 475 (2003).
[5] M. Kozuma, Y. Suzuki, Y. Torii, T. Sugiura, T. Kuga, E. W. Hagley, L. Deng, Science **286**, 2309 (1999).
[6] N. Bar-Gill, E. E. Rowen and N. Davidson, Phys. Rev. A **76**, 043603 (2007).
[7] S. Slama, G. Krenz, S. Bex, C. Zimmermann, Ph. W. Courteille, Phys. Rev. A **75**, 063620 (2007).
[8] L. E. Sadler, J. M. Higbie, S. R. Leslie, M. Vengalattore, and D. M. Stamper-Kurn, Phys. Rev. Lett. **98**, 110401 (2007).
[9] M. G. Moore and P. Meystre, Phys. Rev. Lett. **83**, 5202 (1999).
[10] H. Pu, W. Zhang and P. Meystre, Phys. Rev. Lett. **91**, 150407 (2003).
[11] O. Zobay and G. M. Nikolopoulos, Phys. Rev. A **73**, 013620 (2006).
[12] R. Guo, X. J. Zhou, X. Z. Chen, Phys. Rev. A **78**, 052107

(2008).
[13] O. Zobay and G. M. Nikolopoulos, Laser Physics **17**,180 (2007).
[14] F. Yang, X. J. Zhou, J. T. Li, Y. K, Chen, L. Xia, X. Z. Chen, Phys. Rev. A **78**, 043611 (2008).
[15] M. Cola, L. Volpe and N. Piovella, Phys. Rev. A **79**, 013613 (2009).
[16] N. Piovella, V. Beretta,1 G. R. M. Robb, and R. Bonifacio, Phys. Rev. A **68**, 021801 (2003).
[17] L. Fallani, C. Fort, N. Piovella, M. Cola, F. S. Cataliotti, M. Inguscio, and R. Bonifacio, Phys. Rev. A **71**, 033612 (2005).
[18] J. T. Li, X. J. Zhou, F. Yang, X. Z. Chen, Phys. Lett. A **372**, 4750 (2008).
[19] A. Hilliard, F. Kaminski, R. L. Target, E. S. Polzik, J. H. Müller, arXiv. 0810.5690.
[20] Xu Xu, Xiaoji Zhou, and Xuzong Chen, Phys. Rev. A **79**, 033605 (2009).
[21] G. R. M. Robb and W. J. Firth, Phys. Rev. Lett. **99**, 253601 (2007).
[22] X. J. Zhou, Phys. Rev. A **80**, 023818 (2009).